INSTITUTE OF PHYSICS PUBLISHING PHYSICS IN MEDICINE AND BIOLOGY

Phys. Med. Biol. **48** (2003) 619–632 PII: S0031-9155(03)52022-X

Cryoheater as a means of cryosurgery control

Yoed Rabin and Thomas F Stahovich

Department of Mechanical Engineering, Carnegie Mellon University, Pittsburgh, PA 15213, USA

E-mail: rabin@cmu.edu

Received 6 August 2002
Published 18 February 2003
Online at stacks.iop.org/PMB/48/619

Abstract

A new concept for cryosurgery control is presented in this paper, a concept which has the potential to dramatically change the outcome of cryosurgery. Unlike other cryosurgery control techniques, which are based on controlling the thermal performance of the cryoprobe, this new concept is based on heating the treated tissue as a means of shaping the frozen region. The new controlling heater is termed a 'cryoheater'. The cryoheater is a complementary device to the cryoprobe and can work with any cryosurgery cooling technique. In the current pilot study, the new cryoheater is demonstrated in a gelatin solution and, using heat transfer simulations, it is studied in simulated cases of prostate cryosurgery. It is suggested that cryosurgery planning tools and optimization techniques must be developed before the concept of the cryoheater can be applied in its full capacity.

(Some figures in this article are in colour only in the electronic version)

1. Introduction

Cryosurgery, which is the destruction of undesired tissues by freezing, has been a known surgical treatment since 1845, when James Arnott exposed skin cancer tumours to a partly frozen saline solution, at about −22 °C (Gage 1992). Cryosurgery as an effective treatment of internal organs has been known since 1961, when Cooper and Lee presented the first cryostat for medical applications (Cooper and Lee 1961). The cryostat was defined as a cooling probe in which a cooling sink is generated internally to the probe, known widely today as the 'cryoprobe'. The first cryoprobe was designed to treat brain tumours and the part of the brain associated with Parkinson's disease (Lee 1967). Over the years, cryosurgery has been experimented on a large variety of tumours and other undesired tissues, ranging from brain tumours to tattoo removal. The concept of cryosurgery as a minimally invasive procedure using multiple cryoprobes was formed in the mid 1980s, as a consequence of developments in medical imaging, mainly in ultrasound and magnetic resonance imaging (MRI) (Onik *et al* 1985, 1988, 1993, Gilbert *et al* 1998, Rubinsky *et al* 1993).

Prostate cryosurgery was the first minimally invasive cryosurgical procedure to pass from the experimental stage and become a routine surgical treatment (Onik *et al* 1993). The minimally invasive approach created a new level of difficulty in cryosurgery, in which a well-defined 3D shape of tissue must be treated, while preserving the surrounding tissues. To overcome this difficulty, five (Chang *et al* 1994) and six (Erbe Elektromedizin GmbH, Germany) minimally invasive cryoprobe setups were suggested during the early 1990s, based on liquid nitrogen cooling. With recent technology developments in Joule–Thomson cooling, the diameter of the cryoprobe has been dramatically decreased (Endocare Inc., CA, Galil-Medical Inc., Israel). In order to gain better control over the cryosurgical procedure, the number of cryoprobes has been increased to the point where more than a dozen cryoprobes can be applied simultaneously (Cryoseeds©, Galil-Medical Inc., Israel). Although it is well known that the Joule–Thomson effect generates lower cooling power than liquid nitrogen cooling, as indicated by higher operating temperatures, the lower cooling capabilities are compensated by the increased number of cryoprobes.

With the dramatic increase in the number of cryoprobes, a new challenge has been introduced to cryosurgery, that is, how to shape the frozen region and limit the destructive freezing effect to the target area. A good example of a device that prevents freezing to preserve desired tissues during cryosurgery is the so-called urethral warmer, used in prostate cryosurgery. Technically, the urethral warmer is a counter flow water heat exchanger, embodied in a standard catheter. The water, from a reservoir at close to normal body temperatures, is pumped through the catheter to maintain the urethra temperature above freezing. The urethral warmer has proved to minimize post cryosurgery complications associated with damage to the urethra (Cohen *et al* 1995). Unfortunately, the urethral warmer is the only warmer available today for cryosurgery control, and its heating capabilities are limited (Rabin and Stahovich 2002). Due to its large diameter and insertion technique, it is limited to a specific cryoprocedure.

The purpose of the current paper is to report, for the first time, on a heating device that assists in 3D cryosurgery control using multiple heat sources. (The available urethral warmer is limited to a urethral application, using a single heat source.) The new development is based on a temperature-controlled cartridge heater, termed a 'cryoheater' (Rabin *et al* 1999a). The cryoheater is a complementary device to the cryoprobe, and is independent of the cryoprobe cooling technique. This paper includes: (i) a description of the cryoheater setup, (ii) feasibility testing in a gelatin solution and (iii) a pilot study using computer simulations to demonstrate the use of cryoheaters as a means of cryosurgery control.

2. The cryoheater setup

A schematic illustration of the cryoheater setup is shown in figure 1. The heating element is an electrical resistor, located at the tip of a long hypodermic needle. A temperature sensor is connected to the inner wall of the hypodermic needle, midway between the ends of the electrical heater. Externally, the cryoheater looks similar to the regular minimally invasive cryoprobe, which is in the shape of a long hypodermic needle with a sharp, closed tip.

The cryoheater is connected to a temperature controller with two connectors; one for the temperature sensor, which is used as a feedback for the temperature control mechanism; and one for powering the electrical resistor. The temperature controller is connected to a power supply, which supplies electrical power to the heater when switched on. In concept, the cryoheater is similar to the so-called cartridge heater, widely available for industrial heating applications.

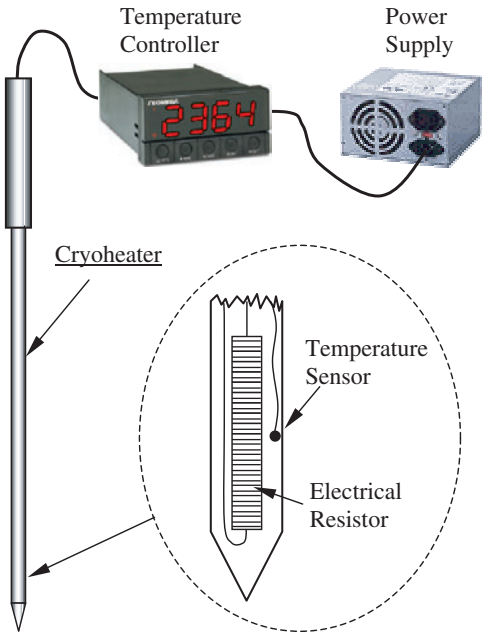

Figure 1. Schematic illustration of the cryoheater setup. The cryoheater has the same external configuration as a standard minimally invasive cryoprobe.

For demonstration purposes, the temperature controller is a laptop computer, measuring temperatures through a usb interface device (OMB55, Omega, Inc.). The switching mechanism is a standard solid-state relay activated by the same usb device. The power supply is a standard ± 5 V/± 12 V power supply harvested from a desktop computer (Bestric Inc., BPS-2004CS-4).

3. Feasibility testing

For the purpose of feasibility testing, a simplified experimental setup has been constructed combining four cryoprobes and one cryoheater, as shown in figure 2. Figure 3(a) shows the relative placement of the heating and cooling components. The plane of the figure is perpendicular to the cryoheater and cryoprobe axes. The cryoprobes have an external diameter of 3 mm and use Joule–Thomson cooling (Galil-Medical, Inc.). The cryoheater is fabricated from a standard electrical resistor wire, wound around a non-conductive core, with an overall electrical resistance of 46 Ω, and an external diameter of 3 mm. The active length of the cryoheater and the effective length of the cryoprobes are all 20 mm.

The container shown in figure 2 is made from 10 mm thick Plexiglas plates, and has internal dimensions of $20 \times 200 \times 200$ mm^3. Note that the width of the container is the same as the active length of the cryoprobes and the cryoheater. Due to the low thermal conductivity of the Plexiglas (about 4% of the conductivity of frozen water), a 2D heat transfer process is expected to develop in the plane perpendicular to the cryoprobes and cryoheater. Since these particular Galil-Medical cryoprobes are not equipped with temperature sensors, external temperature sensors (T type thermocouples) were connected to the cryoprobes, and measured using the same usb interface unit used for control (OMB55, Omega, Inc.). Experiments were performed in a gelatin solution (2.5% by weight) as a phantom material, simulating biological materials. The added gelatin does not significantly affect the thermophysical properties of water.

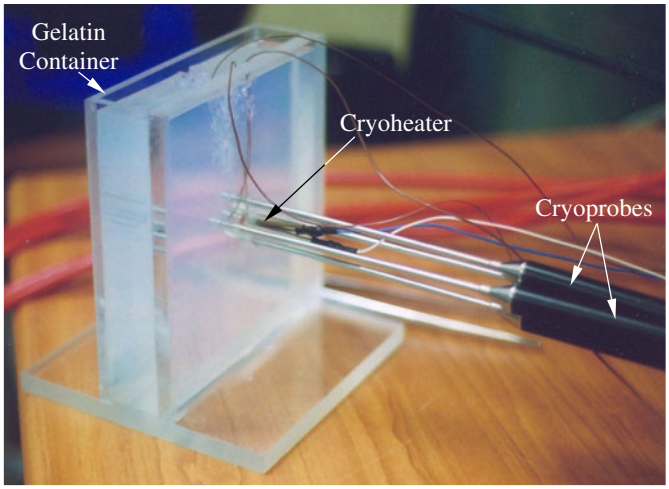

Figure 2. General view of the cryoprobes and cryoheater setup used for feasibility testing. The cryoprobes are of Galil-Medical (Joule–Thomson cooling), having an external diameter of 3 mm. The cryoheater is self-constructed, with an external diameter of 3 mm and active length of 20 mm.

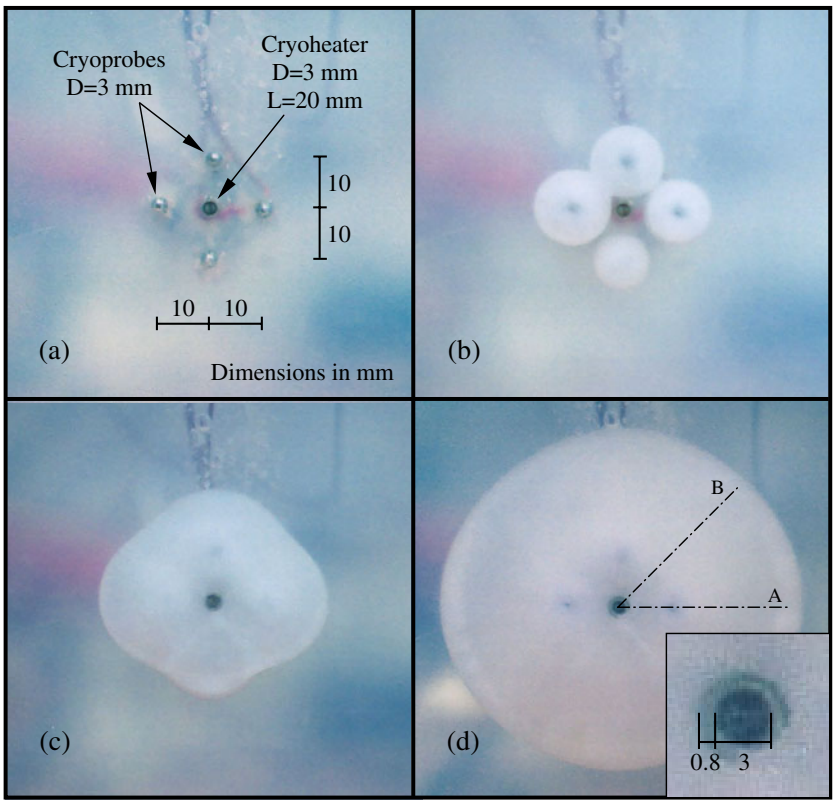

Figure 3. Cross section of the experimental setup before the beginning of the experiment (a), and after 1 (b), 4 (c) and 10 min. (d) From the beginning of experimentation. Radial cross sections A and B refer to the temperature distribution presented in figure 4.

However, the linked gelatin structure prevents convection effects, ensuring that heat transfer prevails solely by conduction, and thus producing a more realistic model of biological tissue.

Figures 3(b)–(d) show the freezing front location after about 1, 4 and 10 min, respectively. It can be seen from figure 3(b) that one cryoprobe (the lower one), has a somewhat lower cooling rate compared to the remaining three, which may represent a typical deviation in the thermal performance of mass production cryoprobes. This deviation in performance has no effect on the feasibility testing, and is addressed in the discussion section. It is interesting to note that nearly perfect cylindrical frozen regions formed along each individual cryoprobe, until the point at which the individual frozen regions started to merge. Figure 3(c) shows the frozen region at a later stage, after the four frozen regions have merged into one, producing an irregularly shaped frozen region. Figure 3(d) shows the frozen region at an advanced stage, where it is nearly a perfect cylinder. Measurements at this stage indicated an average frozen region diameter of 70 mm with a variance of 5% (3.5 mm). This nearly perfect cylindrical region is evidence that the difference in cryoprobe performance seen at the earlier stages of freezing, has no significant effect on the outcome of the cryoprocedure at the advanced stages of the procedure.

The cryoheater was activated prior to the initiation of freezing, with a temperature set point of 37 °C. The effect of heating can clearly be seen in the inset of figure 3(d), where a well-defined unfrozen region, with an average thickness of about 0.8 mm, can be observed around the cryoheater. In a cryosurgical application, this region would be protected from the destructive effect of crystal formation. Note that the long-term destructive effect of freezing is associated not only with freezing, but also with vascular system failure and the wound healing process, which are beyond the scope of this pilot study (Gage and Baust 1998, Rabin *et al* 1999b).

4. Mathematical formulation

In order to analyse the heat transfer observed in the gelatin model, and to perform an initial parametric study of the effect of cryoheaters in cryosurgical applications, a numerical simulation code has been written. The input to the simulation is the cryoprobe and cryoheater temperature protocols, the initial temperature of the gelatin or biological tissue, the geometric dimensions and the physical properties of the gelatin or tissue. The output is the propagation of the freezing front and the temperature distribution as a function of time. The numerical scheme applied in this study has been presented elsewhere (Rabin and Shitzer 1998), and is presented here briefly.

It is customary to assume that heat transfer in the presence of blood perfusion can be modelled by the classical bio-heat equation (Pennes 1948)

$$C\frac{\partial T}{\partial t} = \nabla \cdot (k\nabla T) + w_b C_b (T_b - T) + \dot{q}_{\text{met}} \tag{1}$$

where C is the volumetric specific heat of the tissue, T is the temperature, t is the time, k is the thermal conductivity of the tissue, w_b is the blood perfusion rate (measured in volumetric blood flow rate per unit volume of tissue), C_b is the volumetric specific heat of the blood, T_b is the blood temperature entering the thermally treated area (typically the normal body temperature) and $\dot{q}_{\text{met}}$ is the metabolic heat generation. Note that for blood perfusion, the production of $w_b C_b$ is typically cited in the biothermal literature.

Numerous scientific reports have been published questioning the mathematical consistency of the above classical bioheat heat equation and its validity, while suggesting various alternatives (Wulff 1974, Klinger 1974, Chen 1980, Weinbaum and Jiji 1985). Overviews and discussions regarding these models have been presented by Charny (1992)

Table 1. Representative thermophysical properties of water and frozen biological tissues used in the current analysis (T in K) (Chato 1985, Altman and Dittmer 1971).

Property	Water	Blood
Thermal conductivity, k (W m^{-1} K^{-1})	0.6 $273 < T$ $2135 \times T^{-1.235}$ $T < 273$	0.5 $273 < T$ $15.98–0.0567 \times T$ $251 < T < 273$ $1005 \times T^{-1.15}$ $T < 251$
Volumetric specific heat, C (kJ m^{-3} K^{-1})	4180 $273 < T$ $4.14 \times T$ $T < 273$	3600 $273 < T$ 15 440 $251 < T < 273$ $3.98 \times T$ $T < 251$
Latent heat, L (MJ m^{-3})	330	300
Blood perfusion heating effect, $w_b C_b$ (kW m^{-3} K^{-1})	0	0–40

and Diller (1992). In broad terms, the classical bioheat equation is commonly assumed to be suitable for representing heat flow in the presence of a dense capillary network, and not in the presence of major blood vessels. In fact, the blood perfusion rate is often found by regression of experimental data to theoretical predictions, based on the classical bioheat equation (Rabin *et al* 1996). It is assumed here that a more advanced model of bioheat transfer will not warrant higher accuracy in the cryosurgery simulation but involve greater mathematical complications, and is deemed unnecessary in this pilot study. Note that metabolic heat generation is typically negligible compared to the heating effect of blood perfusion and is neglected in this study (Eberhart 1985).

The scheme used here to solve equation (1) is based on a finite difference formulation

$$T_{i,j,k}^{p+1} = \frac{\Delta t}{\Delta V_{i,j,k}[C_{i,j,k} + (\dot{w}_b C_b)_{i,j,k}\Delta t]} \sum_{l,m,n} \frac{T_{l,m,n}^{p} - T_{i,j,k}^{p}}{R_{l,m,n-i,j,k}} + \frac{\Delta t[(\dot{w}_b C_b)_{i,j,k} T_b + (\dot{q}_{\mathrm{met}})_{i,j,k}] + C_{i,j,k} T_{i,j,k}^{p}}{C_{i,j,k} + (\dot{w}_b C_b)_{i,j,k}\Delta t} \tag{2}$$

where i, j, k and l, m, n are space indexes, p is a time index, ΔV is an element unit volume, Δt is a time interval and R is the thermal resistance to heat transfer between node i, j, k and its neighbour l, m, n. The numerical scheme described in equation (2) is conditionally stable, and a discussion regarding its applicability for cryosurgery has been presented by Rabin and Shitzer (1998).

Table 1 lists typical values of the thermophysical properties of gelatin and biological tissues, which were used in this study. In both, the gelatin experiment and the computer simulations, the cryoheaters were maintained at a nearly constant temperature, equal to the initial temperature of the gelatin or tissue. In the gelatin experiment, the cooling protocol of the cryoprobes could be closely represented by a linear decrease in temperature from the initial temperature of the medium (22 °C for the gelatin) to −145 °C in 30 s. The cyroprobe temperature was nearly constant at −145 °C thereafter. The same protocol was used in the computer simulations.

5. Analysis of the gelatin experiments

Figures 4(a) and (b) present temperature distributions calculated radially from the cryoheater shown in figure 3. Figure 4(a) refers to a cross section that includes the centreline of one of the cryoprobes, such as the cross section A in figure 3(d). Figure 4(b) refers to a cross section

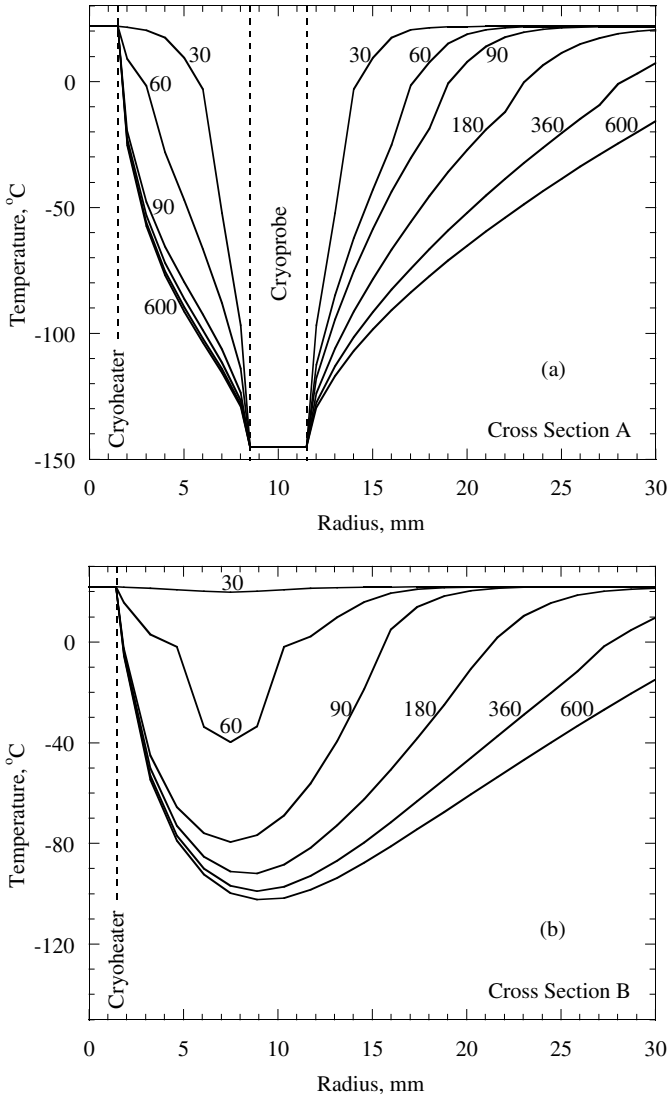

Figure 4. Simulated temperature distribution of the experimental setup measured radially from the cryoheater: (a) in a cross section including one of the cryoprobes (annotated A in figure 3(d)), and (b) in a cross section oriented 45° to the latter cross section (annotated B in figure 3(d)).

oriented 45° to the latter cross section, such as cross section B in figure 3(d). In figure 4, the outer surfaces of the cryoheater and cryoprobe are represented by dashed lines, and the numbers near each curve are the elapsed simulation time in seconds.

It can be seen from figure 4(a) that the temperature distribution in the region between the cryoprobe and the cryoheater reaches steady state rapidly. For example, the temperature distribution at 360 s and 600 s is practically the same. In fact, even the distribution at 180 s differs only insignificantly from that at 600 s. On the other hand, it can be seen that no steady state is achieved at radii larger than the location of the cryoprobe. It can be shown mathematically that, if the heating power of the cryoheater is less than the overall cooling

power of the cryoprobes, there is no steady state solution to the mathematical problem. Note however, that in cryosurgical applications, the heating effect of blood perfusion does limit freezing, even in the absence of a cryoheater.

It can be seen from figure 4(b) that the temperature distribution close to the heater reaches steady state rapidly. However, it can be seen that the temperature distribution is more moderate compared to that presented in figure 4(a). For example, the minimal temperature in cross section B after 600 s is about 40 °C higher than that in cross section A. By comparing subsequent temperature profiles in figure 4(b), it is clear that the minimal temperature in cross section B does not decrease rapidly, and thus this temperature difference will persist. Note that the distance from the cryoheater to the minimal temperature in cross section B is initially much smaller than the distance from the cryoheater to the cryoprobe. However, with time, the former distance approaches the latter. A somewhat irregular temperature distribution is found in cross section B at 60 s. This irregularity originates from the steep change in thermophysical properties of gelatin at phase change, the steep temperature gradient around the cryoprobe and the steep circumferential temperature gradients.

For the gelatin solution, phase transition occurs near 0 °C. However, the phase transition temperature range of biological tissues is typically in the range of −22 °C to 0 °C, assuming that tissues behave thermally like a NaCl solution. Thus, one may argue that the thermal properties of gelatin differ significantly from those of biological tissues, especially during phase transition, and therefore, the feasibility testing may not represent relevant conditions to cryosurgery. However, it has already been demonstrated by Rabin and Korin (1993) that, for the numerical scheme presented in equation (2), the phase transition temperature range has no overall effect on the heat transfer simulation. For this particular formulation, the phase transition temperature-range effect is limited to the vicinity of the phase transition region.

One may further argue that blood perfusion provides a major heating effect, which may make the validity of the above gelatin model questionable. To examine this issue, figures 5(a) and (b) present results of a simulation similar to the gelatin model, but using thermophysical properties typically of biological tissues, and with maximum possible heat generation due to blood perfusion (see table 1). For this simulation, the initial temperature has been modified to 37 °C.

It can be seen from figures 5(a) and (b) that all of the observations made for the gelatin case are also valid for biological tissues. Moreover, the minimal temperature achieved in cross section B is only 5 °C higher for the case of biological tissues, when compared with the gelatin case, where the minimal temperature is about −100 °C.

6. Discussion

Performing feasibility testing using a 2D setup provided many practical advantages. The experimental setup in figure 2 allowed optical observation of both the frozen region formation and the remaining unfrozen region. Such observations are feasible in gelatin experiments, but not under clinical conditions. Furthermore, under clinical conditions, the thin unfrozen cylindrical shell remaining around the cryoheater cannot be observed with available imaging techniques, because the frozen region blocks the signals used by those techniques. Even if modified transducers are developed for this particular task, imaging resolution in layers thinner than 1 mm remains a major barrier.

The experimental setup described in this report could be a somewhat representative thermal model, for example, for a cross section of prostate cryosurgery in the presence of a urethral cryoheater. However, this experimental model falls short of describing the real conditions in the following aspects: (i) In the absence of a heating source, such as

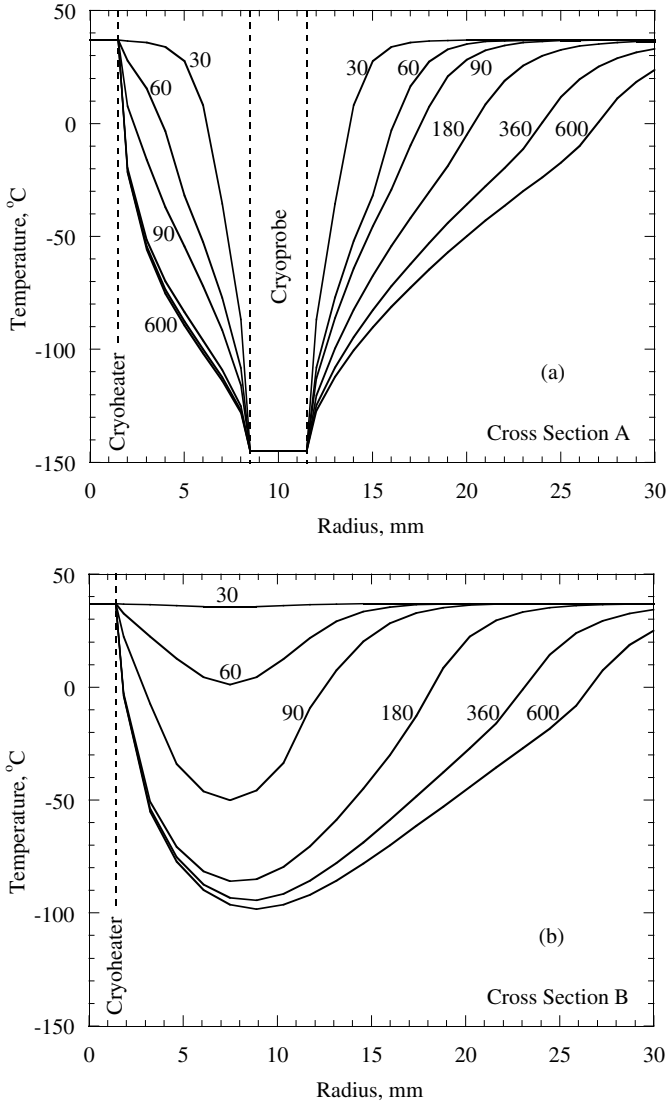

Figure 5. Simulated freezing in a setup similar to figures 2 and 3, with clinically relevant thermophysical properties. Temperature distribution presented radially from the cryoheater: (a) in a cross section including one of the cryoprobes (annotated A in figure 3(d)), and (b) in a cross section oriented 45° to the latter cross section (annotated B in figure 3(d)).

blood perfusion, the freezing process in the experimental setup may never reach steady state. (ii) Modern cryoprobes may be smaller than 3 mm in diameter. (iii) The urethral warmer is typically larger than 3 mm. (iv) The thermal model is two-dimensional while the real process is three-dimensional.

While the experimental setup was designed for feasibility testing only, the discussion below includes more clinically relevant conditions. For this purpose, a 2D parametric study was performed using computer simulation. The details of this parametric study are discussed next, after which the rationale for using a 2D model is presented.

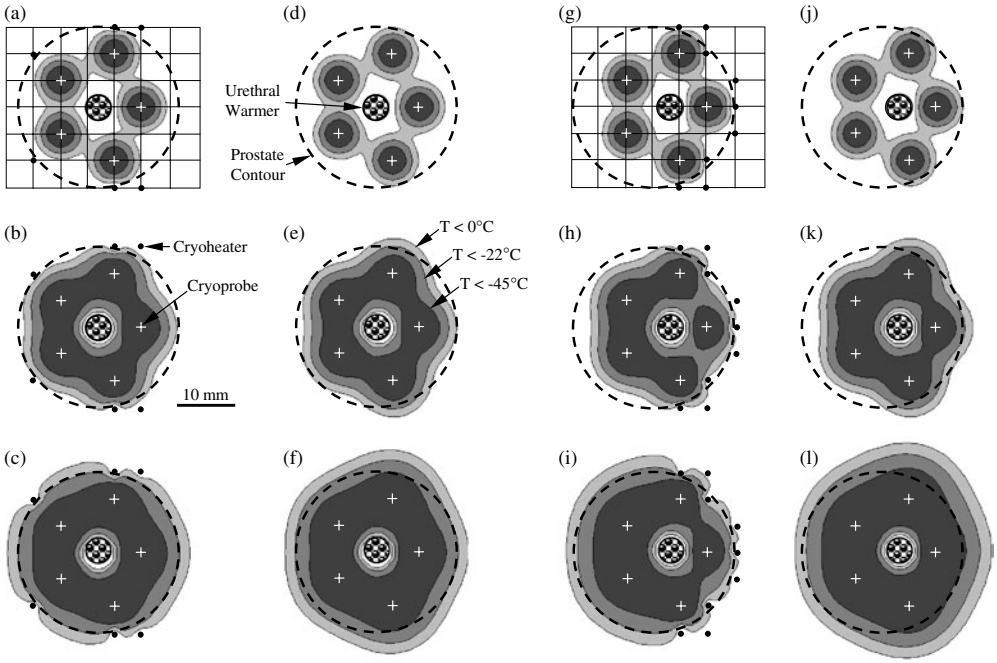

Figure 6. Parametric study of the application of cryoheaters by means of temperature distribution in a 2D process simulating prostate cryosurgery. Four different cases are presented (a)–(c), (d)–(f), (g)–(i) and (j)–(l), described in detail in the text. Four different temperature zones are presented: white for temperatures above freezing, light grey for temperature range from 0 to −22 °C, medium grey for temperature range from −22 to −45 °C and dark grey for temperatures below −45 °C. The plus signs represent cryoprobes and solid circles represent cryoheaters.

It has already been established that blood perfusion conditions can be simulated numerically for typical conditions in cryosurgery. This is even more accurate when the thermal effect of blood perfusion is derived from regression of computer simulations against experimental data (Rabin *et al* 1996). It has also been observed that the rate of growth of the frozen region is not dramatically affected by the rate of blood perfusion (Rabin and Shitzer 1998). Furthermore, the thermal performance of the new element introduced in this study—the cryoheater—is not expected to be affected at all by blood perfusion. This is because blood perfusion can only reduce the amount of heat required from the cryoheater.

Figure 6 presents the results of the parametric study, including four case studies, simulating prostate cryosurgery. A typical prostate ranges from 25 to 50 g (25 to 50 ml). For the purpose of this study, we assume a prostate diameter of about 30 mm and an average length of 35 mm. These dimensions are chosen arbitrarily, within the range of reasonable dimensions, in order to demonstrate the effect of the cryoheater, assuming that a 50 g prostate and a spherical shape would lead to 45 mm in diameter. For case I, the diameter of the urethral warmer is 5 mm, and is located at the centre of the cross section. The diameter of the cryoprobes is 1 mm, which cool from an initial body temperature of 37 °C to a minimal temperature of −145 °C in 30 s. The cryoprobes are localized using a 5 mm grid, similar to the grid used for Cryoseeds (Galil-Medical, Inc.). The diameter of the cryoheaters is 1 mm, with a heating set point of 37 °C. The cryoheaters are compatible with the cryoprobes and localized in a similar manner to the cryoprobes. Case I is schematically

shown in figure 6(a), including the grid, and the 30 mm diameter outer contour of the prostate.

The results for case I after 70, 130 and 230 s of cooling are shown in figures 6(a), (b) and (c), respectively. Three levels of greyscale are used in these figures: dark grey represents temperatures below -45 °C, medium grey represents temperatures between -45 and -22 °C, and light grey represents temperatures between -22 and 0 °C. The unshaded areas represent temperatures above 0 °C. Note that the range from -22 to 0 °C is the assumed phase transition temperature range for biological tissues. Hence, the major destructive effect of crystal formation ends at the lower boundary of this range. However, it is commonly accepted that a lower temperature threshold exists, below which maximal destruction is achieved. This temperature, known as the 'lethal temperature', is commonly accepted to be -45 °C (Gage and Baust 1998).

It can be seen from figure 6(c) that using cryoheaters, the freezing process can be controlled to locate a desired isotherm on the contour of the prostate. In figure 6(c), the -22 °C isotherm is located on the contour. Here, the -22 °C isotherm was chosen for the purpose of demonstration, bypassing the discussion of whether it is best to match 0 °C, -22 °C or -45 °C (lethal temperature) isotherms. For different prostate geometries, the challenge is to select locations for the cryoprobes and cryoheaters so as to control the location of a particular isotherm.

Case II is similar to case I except that cryoheaters are not used. Figures 6(d), (e) and (f) show the various temperature range areas at 70, 130 and 230 s, from the beginning of freezing, respectively. A useful way to compare cases I and II is to compare the areas associated with the three different temperature ranges. In this discussion, maximal prostate area for freezing is taken to be the area within the prostate contour minus the area of the urethral warmer. The goal is to freeze all of the prostate area without freezing the area outside the prostate. In case I, in order to cool 90% of the prostate area below -22 °C, an external area equivalent to 24% of the prostate area has to be cooled below 0 °C, and an external area of 1% cooled below -22 °C. However, in case II an external area equalling 40% must be cooled below 0 °C, and an external area of 12% cooled below -22 °C, in order to achieve the same 90% goal. This represents a major difference in freezing control. Moreover, it can be seen from figure 6(f) that the lethal temperature reaches the prostate contour after 230 s. Any additional cooling will be extremely destructive to the tissue surrounding the prostate.

It is important to note that in cases I and II, the grid placement and location of the cryoprobes and cryoheaters (case I only) were selected so as to minimize the area external to the prostate cooled below 0 °C, while maximizing the area internal to the prostate cooled below -22 °C. Obviously, there is a contradiction between the two criteria. Due to the continuous nature of the temperature field, both criteria cannot be satisfied simultaneously. The current study employed a trial-and-error approach to explore various configurations, and thus the final configuration of cryoprobes and cryoheaters is likely suboptimal. This optimization problem is difficult due to the conflicting nature of the two objectives. The use of cryoheaters simplifies the problem by providing an additional means of controlling the frozen region. Nevertheless, computer-based optimization tools are needed in order to achieve the optimal application of cryosurgery. Such tools are being developed by this research team in the ongoing work, using similar techniques to those presented by Stahovich (2000) and Stahovich and Bal (2002).

Case III is similar in principle to case I except that the urethra is now shifted 3 mm off centre to the right. The urethra is always off centre, away from the large intestine. The ratio of a 3 mm offset to a 30 mm prostate diameter may even be a conservative one. This configuration introduces another level of difficulty because the grid must be shifted to achieve optimal results. Nine cryoheaters are applied in case III. Figures 6(g), (h) and (i) present

results from case III after 70, 130 and 290 s, respectively. Case IV is similar to case III except that cryoheaters are not used. Figures 6(j), (k) and (l) present results from case IV after 70, 130 and 290 s, respectively.

One potential drawback of this new approach may be the large number of cryoheaters required for optimal cryosurgery control of complex geometries. On the other hand, any single cryoheater is expected to improve cryosurgery control, as is evident from figure 6. The application of cryoheaters does not change the physical problem, but makes greater control possible over its solution.

Cryoheaters can be applied so that a thermal barrier may be established, as seen in figure 6(i). Here the temperature field to the right of the urethral warmer has reached steady state while the temperature field to the left of the urethra is still evolving. A similar effect can be observed from the simulation of the gelatin experiment in figures 4(a) and 5(a), in which the temperature distribution between the cryoprobes and the cryoheater reached steady state after about 180 s. Placing such a thermal barrier between the prostate and the large intestine, for example, may be considered advantageous. Such a barrier is not expected to generate any significant artefacts in ultrasound imaging, which is currently done via a rectal ultrasound transducer. A thermal barrier may be even more important when taking into account possible variations in cryoprobe performance such as those shown in figure 3(b). With a thermal barrier, higher cooling power of one of the cryoprobes is less likely to injure important surrounding organs.

Cases I–IV are examples of cryoprocedures in a relatively small area. The small areas are more difficult to control, due to the small number of possible grid points for locating cryoprobes and cryoheaters. Furthermore, the cryoprocedure is more rapid in smaller target areas.

Both the experimental and computational models presented here are two-dimensional. For the gelatin model, the heat transfer is accurately approximated as a 2D process because of the particular geometry and materials used for the container. Most cryosurgical procedures, however, result in 3D heat transfer processes. Nevertheless, 2D models were used here because they still provide useful insights into the use of cryoheaters to control the shape of the frozen region. For example, the 2D models in figure 6 are illustrative of what would occur in a cross section of a prostate during prostate cryosurgery. More discussion with regard to the heating effect of the urethral warmer, based on computer simulations, has been recently presented by Rabin and Stahovich (2002).

Another reason for considering 2D models at this stage is the lack of optimization tools for 3D problems. While it is reasonable to perform manual trial-and-error optimization for the 2D problems in figure 6, manual optimization is not suitable for 3D problems. In 3D processes, the cost of simulation is higher, and it is more difficult to visualize the effects of proposed changes to the configuration, thus making it difficult to use trial-and-error. This observation identifies the next phase of development of multicryoprobe and cryoheater application, which is the development of cryosurgery planning tools. Research is currently under way by this research team to develop such tools.

7. Summary and conclusions

A new concept for cryosurgery control is presented for the first time in this paper. Unlike other cryosurgery control techniques, which are based on controlling the thermal performance of the cryoprobe, the new technology is based on heating as a means of shaping the frozen region. The new controlling heater is termed a ‘cryoheater’. It is acknowledged that some cryoprobes have the ability to heat as a means of controlling the thermal performance of the

cryoprobe. On the other hand, using a cryoprobe solely for heating, for example by means of Joule–Thomson heating, is extremely expensive and thermally inefficient.

An experimental setup has been designed to show the feasibility of using cryoheaters during a simplified simulation of cryosurgery. Thermal analysis has been performed in order to: (i) study the cryoheating effects in the feasibility testing and (ii) demonstrate the control effect in four representative 2D cases, simulating prostate cryosurgery. Based on numerical simulations, it has been shown that the cryoheater concept can dramatically change the outcome of cryosurgery. The four cases chosen for demonstration are in a relatively small target region, where the effect of cryoheaters is expected to be more significant. Another potential application for the cryoheater has been suggested which is forming a thermal barrier along a desired plane.

It is argued that the increasing number of cryoprobes requires development of surgery planning tools, based on numerical optimization. This argument gains more weight with the combination of a large number of cryoprobes and cryoheaters. In the absence of numerical planning and optimization tools, the analysis of 3D cryosurgery involving miniature cryoprobes and cryoheaters seems premature.

References

Altman P L and Dittmer D S 1971 *Respiration and Circulation (Data Handbook)* (Bethesda, MD: Federation of American Societies for Experimental Biology)

Chang Z, Finkelstein J J, Ma H and Baust J 1994 Development of a high-performance multiprobe cryosurgical device *Biomed. Inst. Tech.* **28** 383–90

Charny C K 1992 Mathematical models of bioheat transfer *Advances in Heat Transfer* ed J P Hartnett, T F Irvine and Y I Cho (New York: Academic) pp 19–156

Chato J C 1985 Selected thermophysical properties of biological materials *Heat Transfer in Biology and Medicine* ed A Shitzer and R C Eberhart (New York: Plenum) pp 413–8

Chen M M and Holmes K R 1980 Microvascular contributions in tissue heat transfer *Ann. NY Acad. Sci.* **335** 137–46

Cohen T K, Miller R J and Shumarz B A 1995 Urethral warming catheter for use during cryoablation of the prostate *Urology* **45** 861–4

Cooper I S and Lee A 1961 Cryostatic congelation: a system for producing a limited controlled region of cooling or freezing of biological tissues *J. Nerve Mental Dis.* **133** 259–63

Diller K R 1992 Modeling of bioheat transfer processes at high and low temperatures *Advances in Heat Transfer* ed J P Hartnett, T F Irvine and Y I Cho (New York: Academic) pp 157–358

Eberhart R C 1992 Thermal models of single organs *Heat Transfer in Biology and Medicine* ed A Shitzer and R C Eberhart (New York: Plenum) pp 261–324

Gage A A 1992 Cryosurgery in the treatment of cancer *Surg. Gynecol. Obstet.* **174** 73–92

Gage A A and Baust J 1998 Mechanisms of tissue injury in cryosurgery *Cryobiology* **37** 171–86

Gilbert J, Onik G M and Rubinsky B 1998 MRI guided tissue ablation using cryosurgery *Interventional MR, Techniques and Clinical Experience* ed F A Jolesz and I R Young (New York: Martin Dunitz)

Klinger H G 1974 Heat transfer in perfused biological tissue: I. General theory *Bull. Math. Biol.* **36** 403–18

Lee A S J 1967 Freezing probe for the treatment of tissue, especially in neurosurgery *US Patent* 3, 298, 371

Onik G, Cobb C, Cohen J, Zabkar J and Porterfield B 1988 US characteristics of frozen prostate *Radiology* **168** 629–31

Onik G, Gilbert J, Hoddick W, Filly R, Callen P, Rubinsky B and Farrel L 1985 Sonographic monitoring of hepatic cryosurgery in an experimental animal model AJR Am *J. Roentgenol.* **144** 1043–7

Onik G M, Cohen J K, Reyes G D, Rubinsky B, Chang Z H and Baust J 1993 Transrectal ultrasound-guided percutaneous radical cryosurgical ablation of the prostate *Cancer* **72** 1291–9

Pennes H H 1948 Analysis of tissue and arterial blood temperatures in the resting human forearm *J. Appl. Phys.* **1** 93–122

Rabin Y, Coleman R, Mordohovich D, Ber R and Shitzer A 1996 A new cryosurgical device for controlled freezing II: In vivo experiments on rabbits' hind thighs *Cryobiology* **33** 93–105

Rabin Y, Julian T B, Olson P, Taylor M J and Wolmark N 1999b Long-term follow-Up post-cryosurgery in a sheep breast model *Cryobiology* **39** 29–46

Rabin Y, Julian T B and Wolmark N 1999a Method and apparatus for heating during cryosurgery *US Patent* 5, 899, 897

Rabin Y and Korin E 1993 An efficient numerical solution for the multidimensional solidification (or melting) problem using a microcomputer *Int. J. Heat Mass Trans.* **36** 673–83

Rabin Y and Shitzer A 1998 Numerical solution of the multidimensional freezing problem during cryosurgery *ASME J. Biomech. Eng.* **120** 32–7

Rabin Y and Stahovich T F 2002 The thermal effect of urethral warming during cryosurgery *CryoLetters* **23** 361–74

Rubinsky B, Gilbert J C, Onik G M, Roos M S, Wong S T S and Brennan K M 1993 Monitoring cryosurgery in the brain and the prostate with proton NMR *Cryobiology* **30** 191–9

Stahovich T F 2000 LearnIT: an instance-based approach to learning and reusing design strategies *J. Mech. Design* **122** 249–56

Stahovich T F and Bal H 2002 An inductive approach to learning and reusing design strategies *Res. Eng. Design* **13** 109–21

Weinbaum S and Jiji L M 1985 A new simplified bioheat equation for the effect of blood flow on local average tissue temperature *ASME J. Biomech. Eng.* **107** 131–6

Wulff W 1974 The energy conservation equation for living tissues *IEEE Trans. Biomed. Eng.* **21** 494